

**Influence of impurities on the electronic structure of Y(0001) single-crystal surfaces**

M. Budke\* and M. Donath

*Physikalisches Institut, Westfälische Wilhelms Universität, Wilhelm-Klemm-Strasse 10, 48149 Münster, Germany*

(Received 20 August 2008; published 19 February 2009)

Rare-earth single crystals are known to contain naturally occurring impurities despite fabrication with the best refinement techniques. This is why thin films grown on W(110) or Mo(110) are usually preferred for studies of the surface electronic structure, although the surface order of thin films is generally worse than on single crystals. In this paper, we demonstrate the influence of impurities on the surface electronic structure below and above the Fermi level for different cleaning stages of a Y(0001) single-crystal surface. While the unoccupied electronic structure is only slightly affected by the presence of different impurities, the occupied electronic structure shows characteristic changes depending on the specific impurity at the surface. The nature of the so-called surface-order-dependent state, which has been a source of speculation for more than 20 years, is revealed as a result of a strongly temperature-dependent chemical reaction at the yttrium surface that involves carbon and oxygen. Furthermore, we show that the surface state close to the Fermi energy reacts very sensitively to the surface chemistry. It exhibits an energetic shift that is characteristic of a certain impurity at the surface.

DOI: [10.1103/PhysRevB.79.075432](https://doi.org/10.1103/PhysRevB.79.075432)

PACS number(s): 79.60.Bm, 73.20.At, 71.20.Eh

**I. INTRODUCTION**

The preparation of clean and well-ordered rare-earth surfaces remains a challenge for more than two decades. Ultraviolet-photoemission (PE) spectra from surfaces of bulk single crystals<sup>1,2</sup> (and references therein) are plagued by peaks due to naturally occurring impurities, despite fabrication under the best refinement techniques.<sup>2,3</sup> As a consequence, thin films grown on W(110) and Mo(110) substrates have been preferred over bulk single crystals for studies of the electronic structure because the resulting surfaces are much cleaner.<sup>3</sup> However, defects and/or dislocation lines may be built into the films during the growth process, leading to only poorly ordered surfaces in many cases. This is caused by the different crystal structures of the substrates [body-centered cubic (bcc)] and the overlayers [hexagonally closed-packed (hcp)] and the resulting strain or compression. As a consequence, the obtained surfaces and PE spectra are different from those of single crystals and may substantially differ from preparation to preparation. A prominent example for this dilemma is the ferromagnet gadolinium: while, on the one hand, single-crystal surfaces are practically not suitable for the investigation of the surface electronic structure due to their high level of contaminants, hcp Gd films grown on bcc W(110), on the other hand, exhibit magnetic properties that may vary from sample to sample and depend on the annealing temperature.<sup>4-6</sup>

An alternative to bcc W(110) or Mo(110) substrates is hcp Y(0001). The lattice constant of Y(0001) matches the most heavily studied rare-earth Gd by better than 0.5%. In addition, Y has no *f* electrons, whose spectral signatures could interfere with the signals from the *4f* electrons of Gd. Therefore, Y seems an ideal choice as a substrate for Gd. However, the difficulties with preparing a clean single-crystal surface remain. Studies concerning the magnetic properties of Gd on Y(0001) (Ref. 7) demonstrated that (i) a careful preparation of the Y(0001) substrate is necessary to remove impurities and (ii) a subsequent careful preparation of the Gd film is

essential to avoid intermixing of Gd and Y. A comparison between PE spectra from a Y(0001) single-crystal surface and from Y(0001) thin films<sup>8</sup> shows that intrinsic impurities and unexplained peaks remain in the single-crystal data which are not present in the thin-film data. In particular, an intense feature at about 10 eV binding energy has been a subject of discussion for more than 20 years. Its sensitive dependence on the degree of surface order led to the acronym SODS (surface-order-dependent state) in the literature.<sup>2</sup> The SODS is not only observed on nominally clean Y surfaces but also on Sc, Pr, Gd, Tb, Ho, and Er single-crystal surfaces. However, this feature was never observed on clean thin films of the above elements grown on W(110) or Mo(110) substrates. One reason could have been the lower quality of surface order in these thin films as mentioned above. In a recent Rapid Communication,<sup>9</sup> we were able to show that the SODS feature is in fact due to carbon impurities on the Y surface that form, e.g., upon cooling down the crystal after annealing.

In this paper, we provide a more comprehensive picture of the surface chemistry at the Y(0001) single-crystal surface. We show that the SODS results from a strongly temperature-dependent chemical reaction between carbon and oxygen with yttrium. Further, we demonstrate the influence of chlorine and oxygen impurities on the surface electronic structure for different cleaning stages of the Y crystal. While the unoccupied electronic structure is only weakly influenced by the impurities, very distinct changes are observed in the occupied electronic structure. We have identified the origin of all peaks in the PE spectrum from a Y(0001) single-crystal surface, which allows us to explain the difference between single-crystal and thin-film data. We found that, at elevated temperatures, the spectrum of an Y(0001) single crystal is very similar to that of a thin film of yttrium. Further on, we show that distinct impurities are responsible for adsorbate-induced surface states, which show up at characteristic binding energies similar to oxide-induced states observed for Gd and Lu films.<sup>10</sup>

## II. EXPERIMENT

The experiments were performed in a multichamber ultrahigh-vacuum (UHV) system<sup>11</sup> with separate chambers for sample preparation and analysis at base pressures in the low  $1 \times 10^{-11}$  mbar range. The preparation chamber is equipped with a sputter gun for sample cleaning and techniques for surface characterization such as Auger-electron spectroscopy (AES) and low-energy electron diffraction (LEED). In the analysis chamber, combined PE and inverse-photoemission (IPE) measurements can be performed. A He-gas-discharge lamp is used as light source for PE, providing photon energies of 21.2 eV (He-I) and 40.8 eV (He-II), respectively. The total-energy resolution of the PE system was set to about 50 meV. The IPE experiment is described in detail elsewhere.<sup>12</sup> Briefly, electrons impinge on the sample and undergo radiative transitions into unoccupied electronic states. In our experimental setup, the emitted photons are detected in the isochromate mode by Geiger-Müller counters with a mean detection energy of 9.9 eV. The measurements shown in this article were obtained at a total-energy resolution of 350 meV (full width at half maximum). During the measurements, the sample temperature was varied between 160 and 1100 K. Additionally,  $\text{CO}_2$  and  $\text{O}_2$  can be dosed to the sample via needle valves.

The yttrium single crystal with (0001) surface (Ames National Laboratory) was cleaned for more than 50 h under UHV conditions by repeated sputter/anneal cycles. Sputtering at elevated sample temperatures was also applied. The consequences of different cleaning procedures on the electronic structure and on the level of the different impurities enriched at the surface will be discussed in detail in the following.

## III. RESULTS

### A. Electronic states of an as-prepared Y(0001) single-crystal surface: overview

In a first attempt to obtain a clean surface, the sample was sputtered for 10 min with 1 keV  $\text{Ar}^+$  ions (sample current  $\approx 5 \mu\text{A}$ , angle of incidence  $30^\circ$ ). Then, the sample was annealed to 950 K for 30 min. This procedure was repeated more than 30 times. Figure 1 shows angle-resolved PE and IPE measurements obtained from the Y(0001) single-crystal surface after this cleaning procedure. Please note PE and IPE measurements obtained at the same angles of emission and incidence, yet with different photon energies, probe electronic states at different  $\mathbf{k}_\parallel$ .

In good agreement with previous IPE measurements on Y(0001),<sup>13</sup> three weakly dispersing features can be identified at energies of 0.6, 2.2, and 4 eV above the Fermi level. In the PE spectra, six nondispersing spectral features are observed. Note that for Y(0001) thin films a surface-state emission is observed at  $-0.2$  eV at room temperature.<sup>8</sup> In contrast, no such feature can be observed in the PE spectra of Fig. 1. The rather weak feature at  $-0.7$  eV represents an oxygen-induced surface state (see Sec. III D). The broad feature at  $-2$  eV is partly attributed to a bulk-band transition as identified in previous studies of Y thin films.<sup>8</sup> The peak at  $-4$  eV

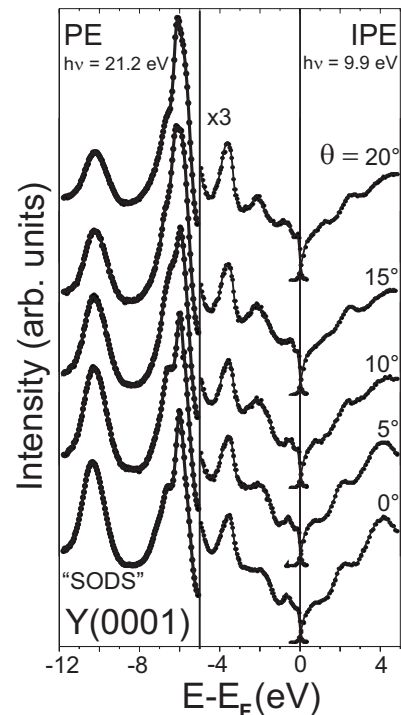


FIG. 1. Angle-resolved PE and IPE spectra for an as-prepared Y(0001) surface along  $\bar{\Gamma}\bar{M}$ .

is caused by hydrogen contamination. The same feature was identified in hydrogen adsorption experiments on Gd(0001).<sup>14</sup> The intense spectral feature at  $-6$  eV is caused by yttrium oxides. A similar, yet much broader structure was found in oxygen adsorption experiments on Gd(0001) and assigned to  $\text{Gd}_2\text{O}_3$ .<sup>10</sup> The peak appeared much sharper, when the Gd surface was annealed to 345 K after oxygen exposure. Additionally, an exchange-split surface state was found at about  $-0.7$  eV, which was attributed to a magnetically ordered surface oxide on Gd. At first sight, the high level of oxygen contamination on our Y crystal is rather surprising because no oxygen could be detected on the surface by AES after the preparation procedure. However, it should be noted that the surface was still warm during the AES measurements. In fact, PE measurements on Y(0001) held at a temperature of 1100 K showed a much smaller oxygen-induced spectral feature, indicative of a lower level of oxygen contamination.<sup>9</sup> In addition, on the hot Y(0001) crystal surface, the surface-state emission was observed at  $-0.2$  eV with high intensity as on the thin-film surface.

An additional peak at about  $-7$  eV is implied as a shoulder in the intense structure at  $-6$  eV. As will be shown later, this peak can be assigned to chlorine impurities. Finally, at about  $-10$  eV, one more intense spectral feature is clearly visible. This peak is found in a similar way on many other rare-earth single-crystal surfaces and was labeled surface-order-dependent state (SODS) due to its sensitivity to the degree of surface crystalline order. It was shown recently<sup>9</sup> that the SODS is in fact due to carbon contamination. This will be elaborated by comprehensive adsorption experiments in the following.

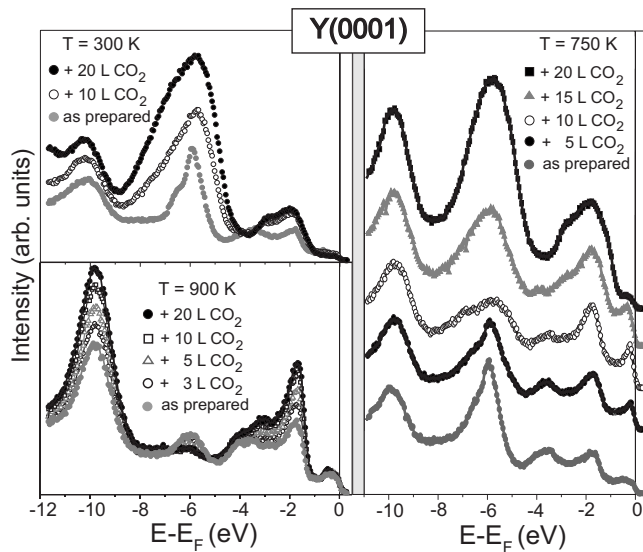


FIG. 2. Adsorption experiments with  $\text{CO}_2$  performed on the Y(0001) single crystal at temperatures of 300, 750, and 900 K. The PE spectra ( $h\nu=21.2$  eV, normal emission) were obtained during  $\text{CO}_2$  exposure of up to 20 L (1 L =  $1 \times 10^{-6}$  Torr  $\times$  s).

### B. Surface-order-dependent state

We investigated the origin of the SODS in detail by adsorption experiments with  $\text{CO}_2$  at different sample temperatures. Our PE results for sample temperatures of 300, 750, and 900 K are summarized in Fig. 2. In all three cases, we started with a sample preparation that results in an intense oxygen-induced PE feature at  $-6$  eV as well as a considerable SODS at about  $-10$  eV (see Fig. 1). For each series of spectra, the sample was held at a fixed temperature and the PE spectra were recorded, while the surface was exposed to  $\text{CO}_2$ . In this way, the changes in the spectra could be followed immediately. Each series consists of about 40 spectra. Figure 2 displays selected spectra for certain  $\text{CO}_2$  exposures. At a sample temperature of 300 K, the exposure to  $\text{CO}_2$  causes an increase in an intense broad feature between  $-4$  and  $-8$  eV and a decrease in intensity at the Fermi level. A CO adsorption experiment on Gd(0001) (Ref. 14) resulted in similar effects that were interpreted in terms of  $\text{Gd}_2\text{O}_3$  formation. Since the valence electronic structure of Gd and Y is very similar, we conclude that the reduced spectral intensity at the Fermi level points to the formation of insulating  $\text{Y}_2\text{O}_3$ . An electron transfer from Y to O causes a reduced conductivity at the surface. Additionally, the  $\text{CO}_2$  dosage leads to the rise of a broad double-peaked structure around  $-2$  eV. This is also in line with observations on Gd(0001), where these peaks are attributed to carbon compounds.<sup>14,15</sup> The reaction of the SODS upon  $\text{CO}_2$  exposure can hardly be judged because of the broad oxygen-induced structure and the changing background.

The situation changes drastically when the same experiment is performed at 900 K. At this temperature, the oxygen peak at  $-6$  eV is strongly reduced in intensity already for the as-prepared sample. Upon  $\text{CO}_2$  dosage, it further loses intensity, while the intensity at the Fermi level becomes slightly enhanced and the SODS as well as a peak at  $-2$  eV strongly

gain intensity. Furthermore, a peak at  $-3.2$  eV emerges with similar intensity as for 300 K. In summary, at 900 K the formation of sesquioxides is suppressed, and the rise of the SODS upon  $\text{CO}_2$  dosage clearly reveals its origin as due to carbon impurities.

However, it still remains unclear what happens to the oxygen-induced peak at  $-6$  eV. Its behavior can be investigated more clearly at a sample temperature of 750 K, where the peak at  $-6$  eV still has considerable intensity. When up to 10 L of  $\text{CO}_2$  are dosed to the surface, the peak at  $-6$  eV clearly loses intensity and broadens. Parallel to this, the SODS only slightly gains intensity and shifts by about 200 meV to lower binding energy, whereas the peak at  $-2$  eV strongly emerges. Note that there is no peak at  $-3.2$  eV visible up to this point. Furthermore, the surface-state emission shows up clearly at  $-0.2$  eV. This points to the conclusion that the surface becomes cleaner during  $\text{CO}_2$  exposure of up to 10 L. In fact, these observations lead to the assumption that oxygen is leaving the surface. When, however, more  $\text{CO}_2$  is dosed to the surface, a broad oxygen-induced structure appears, pointing to  $\text{Y}_2\text{O}_3$  formation, whereas the surface state is completely quenched. When increasing the  $\text{CO}_2$  exposure from 10 to 20 L, the SODS increases in intensity much more than for the first 10 L of  $\text{CO}_2$  and, at the same time, the peak at  $-3.2$  eV rises. Therefore, we assume that this peak is related to the SODS. The peak at  $-2$  eV, however, only slightly gains intensity.

### C. Combined PE/IPE and AES results of different cleaning stages

All adsorption experiments suffered from the restriction that it was not possible to prepare the surface with one adsorbate or impurity at a time. The unavoidable interplay between segregation of bulk impurities to the surface and adsorption of defined gas molecules at the surface complicates the interpretation of our results. To further clarify the influence of different impurities on the PE spectra obtained from an Y(0001) single-crystal surface, we combined PE with AES measurements. The results are shown in Fig. 3. Note that the sample temperature was 295 K during all measurements except for the bottom spectra. The topmost PE and AES results were obtained after exposure to 20 L  $\text{CO}_2$  at 900 K. The Auger spectrum shows the characteristic Y transitions between 50 and 150 eV and a significant carbon peak at 271 eV. Further, a small oxygen peak can be observed at about 500 eV. Upon cooling down to room temperature after  $\text{CO}_2$  exposure at 900 K, we observed a steady rise of the oxygen-induced PE feature. At room temperature, the level of oxygen contamination is significantly higher (see topmost PE spectrum in Fig. 3) than immediately after  $\text{CO}_2$  exposure at 900 K (see corresponding spectrum in Fig. 2). Note that at room temperature, the spectrum of this carbonated Y surface remained unchanged for days under UHV conditions, indicative for a stable inert surface.

The second spectra from the top in Fig. 3 display PE and AES results for an oxygen-contaminated surface as obtained after sputter-anneal-cycles as described in Sec. III A. In contrast to the spectra shown in Fig. 1, no SODS feature is

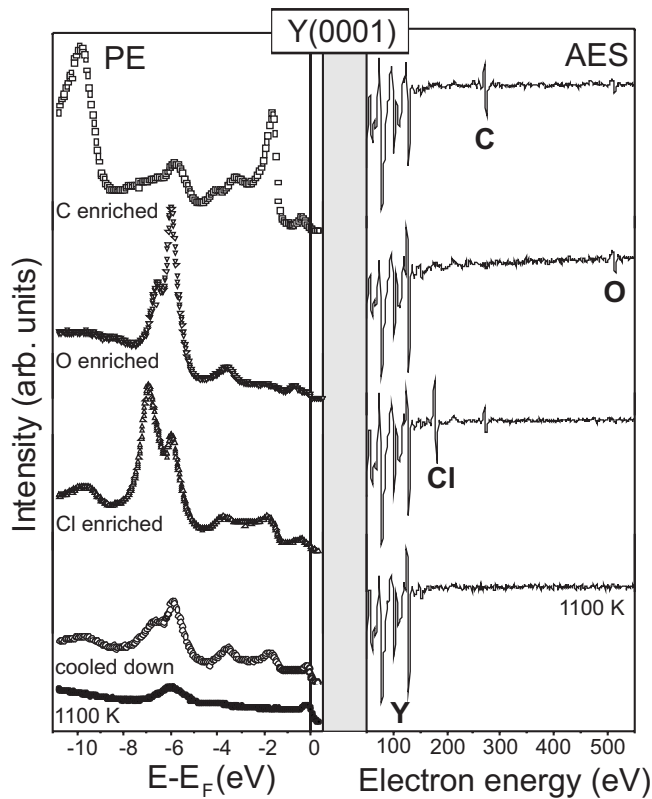


FIG. 3. Photoemission ( $h\nu=21.2$  eV, normal emission) and corresponding Auger-electron spectra of different cleaning stages of a Y(0001) single crystal (see text for details). Hydrogen, oxygen, chlorine, and carbon impurities lead to peaks in the photoemission spectra at energies of  $-4$ ,  $-6$ ,  $-7$ , and  $-10$  eV, respectively. When the yttrium sample is heated to 1100 K, all impurity-induced features (except a residual oxygen peak) are quenched. The corresponding Auger spectrum represents a clean Y surface without contaminations.

found in this spectrum. It should be noted that the intensity of the SODS feature strongly depends on the history of cleaning cycles before a PE measurement. We found that repeated sputter cycles with moderate annealing temperatures of about 800 K lead to a depletion of carbon impurities in the near-surface region and, consequently, to a quenching of the SODS feature. The only contamination that can clearly be identified in the corresponding Auger spectrum is oxygen.

In a further cleaning step, we increased the annealing temperature to 1100 K. The sputter parameters and the annealing time were kept as described above. The result of the increased annealing temperature is an enrichment of chlorine and carbon impurities on the surface. The third spectra from the top in Fig. 3 represent the corresponding PE and Auger results. An intense chlorine peak and a carbon peak are clearly visible in the Auger spectrum. Note that the AES sensitivity for chlorine is much higher than for carbon so the peak intensities cannot be compared directly. The PE spectrum shows an intense peak due to chlorine at  $-7$  eV. Additionally, the oxygen peak at  $-6$  eV is visible but with lower intensity compared with the above cleaning attempt using moderate annealing temperatures. Furthermore, the SODS feature is visible at about  $-10$  eV, indicative of carbon con-

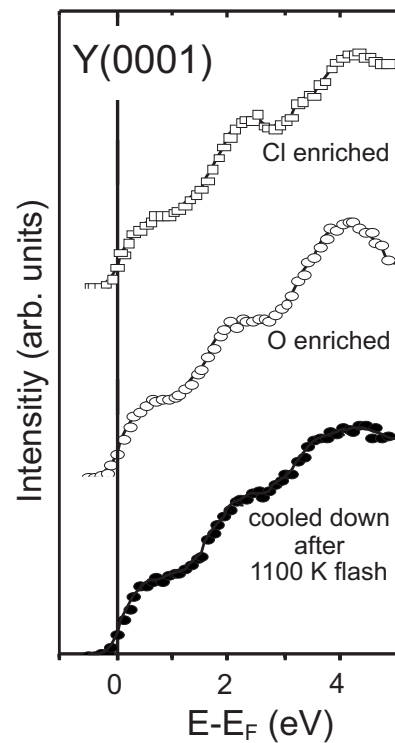


FIG. 4. IPE spectra ( $h\nu=9.9$  eV, normal incidence) obtained from the Cl-enriched surface (open squares), the O-enriched surface (open dots), and from the Y(0001) surface cooled down immediately after a 1100 K flash (filled dots).

tamination. In further cleaning cycles, it was possible to reduce the level of Cl impurities in the near-surface region by reducing the sputter time by 50% under otherwise unchanged conditions. However, due to the high annealing temperature, the level of carbon impurities steadily increased.

The bottom spectra shown in Fig. 3 were obtained from the Y(0001) crystal after depletion of Cl impurities in the near-surface region while the crystal was held at a temperature of 1100 K. The corresponding Auger spectrum does not show any contamination. In the PE spectrum, all impurity-related peaks are completely quenched except a small oxygen-induced feature. However, the surface state at the Fermi energy is enhanced in intensity and shows up at the same binding energy as in experiments performed on Y thin films.<sup>8</sup> Note, that in PE measurements with a photon energy of 40.8 eV (He-II), the surface state appears with strongly enhanced intensity,<sup>9</sup> showing perfect agreement with the thin-film data.<sup>8</sup> However, when the crystal cools down, all of the above mentioned impurities return, especially the oxygen-induced peak at  $-6$  eV (second spectrum from the bottom in Fig. 3). Simultaneously, the surface-state intensity at  $-0.2$  eV is reduced.

Figure 4 shows IPE results for Cl- and O-contaminated Y surfaces as well as for the clean surface immediately after the 1100 K flash. Surprisingly, in contrast to the PE spectra shown in Fig. 3, the IPE spectra do not clearly reflect the impurity level. While all IPE spectra show three features at 0.6, 2.2, and 4 eV, the intensity of the peak at 4 eV is strongest for the O-enriched surface. This led us to the assumption that the peak at 4 eV may be somehow related to the presence of oxygen on the surface.

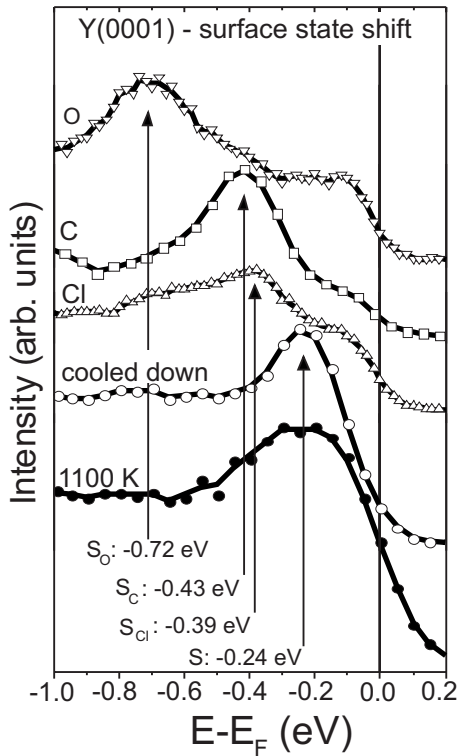


FIG. 5. Near Fermi-energy region enlarged from the spectra shown in Fig. 3. The enrichment of different impurities leads to the formation of impurity-induced surface states at characteristic energies of  $-0.72$ ,  $-0.43$  eV, and  $-0.39$  eV for oxygen, carbon, and chlorine, respectively. The surface-state emission from clean Y(0001) is observed at  $-0.24$  eV.

#### D. Adsorbate-induced surface states

There is another interesting point to be learned from the PE spectrum of the hot Y surface shown in Fig. 3: The surface state just below the Fermi energy appears (as on the thin film) at about  $-0.2$  eV and not shifted to somewhat higher binding energies as in the other spectra shown in Fig. 3. We have to emphasize that, close to  $E_F$ , the observed peak energies may not necessarily reflect the true binding energies of the electron states due to temperature-dependent broadening of the Fermi cutoff in combination with a finite-energy resolution.<sup>11</sup> To get a more detailed view of the surface-state energies, the near Fermi-energy region of the spectra of Fig. 3 is shown on an enlarged energy scale in Fig. 5. Only the spectra taken at 1100 K and immediately after cooling reproduce the surface-state binding energy of the thin-film spectrum. In fact, we observed that the surface-state emission at  $-0.2$  eV was completely quenched within about 1 h after cooling down. Parallel to the loss in intensity at  $-0.2$  eV, we saw an increase in the impurity-induced peaks between  $-4$  and  $-10$  eV, especially at  $-6$  eV caused by the main impurity oxygen. In the spectrum labeled “cooled down,” a peak at  $-0.7$  eV starts to appear. Interestingly, the surface-state emission at  $-0.2$  eV and the emerging peak at  $-0.7$  eV can be observed simultaneously on the surface (second spectrum from the bottom, Fig. 5). An oxygen-enriched surface only shows the peak at  $-0.7$  eV (top spectrum in Fig. 5) while the

TABLE I. Summary of impurities, associated peak energies in the PE spectra at normal emission, and impurity-induced surface-state emission. The clean Y(0001) surface only shows a bulk-band transition at  $-2$  eV and a surface-state emission at about  $-0.2$  eV.

| Impurity              | Associated peak energy          | Impurity-induced surface-state energy |
|-----------------------|---------------------------------|---------------------------------------|
| Carbon                | $-10$ eV                        | $-0.43$ eV                            |
| Chlorine              | $-7$ eV                         | $-0.39$ eV                            |
| Oxygen                | $-6$ eV                         | $-0.72$ eV                            |
| Clean Y(0001) surface | Surface state at $\sim -0.2$ eV | Bulk states at $\sim -2$ eV           |

“true” Y surface state is not visible. We interpret the peak at  $-0.7$  eV as oxygen-induced surface state. However, it is not simply molecular or dissociated oxygen that is responsible for the peak at  $-0.7$  eV but rather yttrium oxides. This is suggested by an adsorption experiment with oxygen performed at room temperature that led to a quenching of the peak at  $-0.7$  eV (not shown). Note, that oxide-induced surface states are also observed on Gd and Lu(0001) films.<sup>10</sup> In these experiments, 1 L oxygen was dosed to the surface, then the films were annealed to 345 and 700 K, respectively. As in the forecited article, we exclude the involvement of yttrium sesquioxides due to the remaining considerable intensity at the Fermi level reflecting the metallic character of the surface. Instead, the oxidized surface represents well-ordered YO compounds with a sharp ( $1 \times 1$ ) LEED pattern.

We also found characteristic surface-state energies for the other main impurities, chlorine and carbon. While on the chlorine-enriched surface (third spectrum from the top in Fig. 5), both a chlorine-induced peak at  $-0.39$  eV and the oxide-induced surface state at  $-0.7$  eV are visible; the carbon-enriched surface (second spectrum from the top) exhibits only one intense feature at  $-0.43$  eV. The reason is the much lower level of oxygen contamination as reflected by the low intensity of the  $-6$  eV peak in the corresponding spectrum in Fig. 3. The fact that several impurity-induced surface states can be observed together in the same spectrum can be explained by the strong localization of the  $d_{z^2}$ -like surface state. As a consequence, an independent existence of the different surface states is possible in different regions of the sample surface. Since photoemission integrates over a macroscopic area, the resulting spectra may show more than one surface state.

#### IV. CONCLUSION

In this paper, we investigated the effects of impurities, caused by segregation and/or adsorption, on the surface electronic structure of Y(0001) single-crystal surfaces. Our photoemission results for different cleaning stages of the single crystal are summarized in the table shown in Table I. By performing combined PE/AES measurements we were able to identify the origin of all peaks present in the photoemission data. Especially, we provided evidence that the so-called surface-order-dependent state is due to carbon impurities. In

addition, we demonstrated that, depending on the impurity being enriched in the cleaning process, characteristic surface states near the Fermi energy appear, whose binding energies are characteristic of the enriched impurity. We have further shown that all observed impurities, except a small amount of oxygen, are desorbed from the surface at a temperature of 1100 K. At this temperature, the photoemission spectrum is fully consistent with the data obtained from thin Y(0001) films.

It remains the question about the suitability of Y(0001) single crystals as substrates for rare-earth thin films, e.g., Gd. On the one hand, the identical crystal structure with only small lattice mismatch promises a well-ordered crystalline structure. On the other hand, this study has shown that it is highly sophisticated to reach a simultaneous depletion of C,

Cl, and O impurities in the near-surface region of Y(0001) by conventional sputter/anneal cycles. Therefore, it has to be taken into account that thin Gd films grown on Y(0001) single crystals may be influenced by substrate impurities. Future studies of Gd/Y(0001) will have to show whether Y(0001) is nevertheless suitable as a substrate for the preparation of high-quality Gd(0001) films.

#### ACKNOWLEDGMENTS

Enjoyable collaboration with T. Allmers and J. S. Correa as well as financial support by the Deutsche Forschungsgemeinschaft through the priority program SP1133 is gratefully acknowledged.

---

\*Corresponding author; mbudke@arcor.de

<sup>1</sup>D. E. Eastman, *Solid State Commun.* **7**, 1697 (1969).

<sup>2</sup>S. D. Barrett, *Surf. Sci. Rep.* **14**, 271 (1992).

<sup>3</sup>M. Bodenbach, A. Höhr, C. Laubschat, G. Kaindl, and M. Methfessel, *Phys. Rev. B* **50**, 14446 (1994).

<sup>4</sup>D. P. Pappas, C. S. Arnold, and A. P. Popov, in *Magnetism and Electronic Correlations in Local-Moment Systems*, edited by M. Donath, P. A. Dowben, and W. Nolting (World Scientific, Singapore, 1998).

<sup>5</sup>S. D. Barrett and S. S. Dhesi, *The Structure of Rare-Earth Metal Surfaces* (Imperial College Press, London, 2001).

<sup>6</sup>E. D. Tober, R. X. Ynzunza, C. Westphal, and C. S. Fadley, *Phys. Rev. B* **53**, 5444 (1996).

<sup>7</sup>S. R. Mishra, T. R. Cummins, G. D. Waddill, K. W. Goodman, J. G. Tobin, W. J. Gammon, T. Sherwood, and D. P. Pappas, *J. Vac. Sci. Technol. A* **16**, 1348 (1998).

<sup>8</sup>R. I. R. Blyth, C. Searle, N. Tucker, R. G. White, T. K. Johal, J.

Thompson, and S. D. Barrett, *Phys. Rev. B* **68**, 205404 (2003).

<sup>9</sup>M. Budke, J. S. Correa, and M. Donath, *Phys. Rev. B* **77**, 161401(R) (2008).

<sup>10</sup>C. Schüßler-Langeheine, R. Meier, H. Ott, Z. Hu, Chandan Mazumdar, A. Yu. Grigoriev, G. Kaindl, and E. Weschke, *Phys. Rev. B* **60**, 3449 (1999).

<sup>11</sup>M. Budke, T. Allmers, M. Donath, and G. Rangelov, *Rev. Sci. Instrum.* **78**, 113909 (2007).

<sup>12</sup>M. Budke, V. Renken, H. Liebl, G. Rangelov, and M. Donath, *Rev. Sci. Instrum.* **78**, 083903 (2007).

<sup>13</sup>R. I. R. Blyth, P. T. Andrews, and S. D. Barrett, *J. Phys.: Condens. Matter* **3**, 2827 (1991).

<sup>14</sup>M. Getzlaff, M. Bode, R. Pascal, and R. Wiesendanger, *Phys. Rev. B* **59**, 8195 (1999).

<sup>15</sup>C. Searle, R. I. R. Blyth, R. G. White, N. P. Tucker, M. H. Lee, and S. D. Barrett, *J. Synchrotron Radiat.* **2**, 312 (1995).